

RESEARCH ARTICLE | APRIL 01 2025

Spontaneous single-molecule dissociation in infrared nanocavities

Special Collection: 2024 JCP Emerging Investigators Special Collection

Johan F. Triana   ; Felipe Herrera 

 Check for updates

J. Chem. Phys. 162, 134103 (2025)

<https://doi.org/10.1063/5.0247008>



Articles You May Be Interested In

The shape of the electric dipole function determines the sub-picosecond dynamics of anharmonic vibrational polaritons

J. Chem. Phys. (June 2020)

Scanning a photonic crystal slab nanocavity by condensation of xenon

Appl. Phys. Lett. (September 2005)

Position dependent optical coupling between single quantum dots and photonic crystal nanocavities

Appl. Phys. Lett. (August 2016)



Nanotechnology &
Materials Science



Optics &
Photonics



Impedance
Analysis



Scanning Probe
Microscopy



Sensors



Failure Analysis &
Semiconductors



Unlock the Full Spectrum.
From DC to 8.5 GHz.

Your Application. Measured.

[Find out more](#)

 Zurich
Instruments

Spontaneous single-molecule dissociation in infrared nanocavities

Cite as: *J. Chem. Phys.* **162**, 134103 (2025); doi: 10.1063/5.0247008

Submitted: 5 November 2024 • Accepted: 15 March 2025 •

Published Online: 1 April 2025



View Online



Export Citation



CrossMark

Johan F. Triana^{1,a)}  and Felipe Herrera^{2,3,b)} 

AFFILIATIONS

¹ Department of Physics, Universidad Católica del Norte, Av. Angamos, 0610 Antofagasta, Chile

² Department of Physics, Universidad de Santiago de Chile, Av. Victor Jara, 3493 Santiago, Chile

³ ANID-Millennium Institute for Research in Optics, Santiago, Chile

Note: This paper is part of the 2024 JCP Emerging Investigators Special Collection.

a) Author to whom correspondence should be addressed: johan.triana@ucn.cl

b) Electronic mail: felipe.herrera.u@usach.cl

ABSTRACT

Ultrastrong light-matter interaction with molecular vibrations in infrared cavities has emerged as a tool for manipulating and controlling chemical reactivity. By studying the wavepacket dynamics of an individual polar diatomic molecule in a quantized infrared electromagnetic environment, we show that chemical bonds can efficiently dissociate in the absence of additional thermal or coherent energy sources, provided that the coupled system is prepared in a suitable diabatic state. Using hydrogen fluoride as a case study, we predict dissociation probabilities of up to 35% in less than 200 fs for a vibration-cavity system that is rapidly initialized with a low number of bare vibrational and cavity excitations. We develop a simple and general analytical model based on the multipolar formulation of quantum electrodynamics to show that the Bloch-Seigert shift of the bare vibrational ground state is a predictor of a threshold coupling strength below which no spontaneous dissociation is expected. The role of state-dependent permanent dipole moments in the light-matter interaction process is clarified. Our work paves the way toward the development of vacuum-assisted chemical reactors powered by ultrastrong light-matter interaction at the single-molecule level.

Published under an exclusive license by AIP Publishing. <https://doi.org/10.1063/5.0247008>

I. INTRODUCTION

The manipulation of strong light-matter coupling in confined electromagnetic environments has enabled applications in precision measurements,¹ quantum information processing,² and quantum optics.³ As the interaction strength approaches the ultrastrong coupling (USC) regime,^{4,5} light and matter degrees of freedom become significantly modified relative to free space,^{6,7} as demonstrated with semiconductors,⁸ superconducting circuits,⁹ and organic microcavities.^{10–12} Recent breakthroughs in nanophotonics have enabled the demonstration of strong and ultrastrong coupling between an individual molecule and a plasmonic field, by stabilizing the confined field of a localized plasmon resonance in the optical regime to a few cubic nanometers.^{13–16} Emerging materials with tunable plasmonic resonances can also be used to produce strong field confinements in the mid-infrared spectral region,^{17–19} which could enable studies of quantum light-matter interaction using

high-frequency intramolecular vibrations at the single-molecule level.²⁰

Anharmonic vibrational polaritons in strong and ultrastrong coupling can be studied using a fully-retarded multipolar formulation of quantum electrodynamics (QED).^{21–27} Multipolar QED describes light-matter interaction in terms of electric and magnetic field operators and is unitarily equivalent to the minimal coupling formulation via a Power-Zienau-Woolley (PZW) transformation.²⁸ Gauge invariance of the PZW transformation was first demonstrated in 1970,²² revisited more recently in Refs. 25 and 26 and generalized in Ref. 28. Ignoring the continuous multimode nature of the electromagnetic vector field in canonical quantization procedures can lead to physical inconsistencies such as the breakdown of gauge invariance with respect to minimal coupling^{29–31} and superluminal signal propagation.³² *Ad hoc* unitary transformations can be constructed to fix these issues in single-mode field theories.^{33,34}

Another approach to cavity QED is the Pauli–Fierz model, advocated for molecular systems in Refs. 35 and 36. This model Hamiltonian derives from a mode-truncated minimal coupling form through a mode-truncated PZW unitary transformation.³⁷ Like other mode-truncated cavity QED models, the Pauli–Fierz Hamiltonian also suffers from superluminal signal propagation.³² However, for cavity setups where the speed of light can be considered infinite over the relevant system timescales, light propagation can be ignored and the focus can be placed on the light–matter eigenvalues and eigenstates. One often discussed feature of the Pauli–Fierz model is the tensorial character of its dipole self-energy term,^{38,39} which scales linearly with the vacuum field fluctuation $\langle \hat{E}_0^2 \rangle$ to preserve gauge invariance at an equivalent level of mode truncation.³⁷ \hat{E}_0 is the electric field operator of the discrete cavity mode. This field-dependent dipole self-energy, as opposed to a field-free self-energy in multipolar QED, could become dominant in ultrastrong coupling, with physical consequences that so far have not been seen in existing USC implementations.^{40,41}

We use the multi-level quantum Rabi (MLQR) model^{6,7} to study vibrational polaritons in the coordinate representation. The MLQR model derives from the fully retarded gauge-invariant multipolar QED Hamiltonian,^{25,28} with the polarization density truncated up to dipole terms. The model has been used to understand the role of vibrational permanent dipole moments in polarizing the cavity field⁷ and to model nonlinear infrared cavity spectroscopy of polar nitroprusside molecules.¹⁹ In the MLQR model, the dipole self-energy is *independent* of the vacuum field amplitude and polarization, and only gives perturbative corrections to the molecular energy levels that can be evaluated with standard QED techniques.^{42,43} For nonpolar molecules, the MLQR and Pauli–Fierz models give equivalent predictions for spectroscopic and dynamical observables in strong coupling.^{44–47} However, the two approaches can differ substantially in ultrastrong coupling,³⁶ particularly for molecules with permanent dipole moments. Comparisons in the Pauli–Fierz and Multipolar QED models for vibrational polaritons in USC can be found in Refs. 36 and 48.

In this work, we study the dissociation dynamics of a single hydrogen fluoride (HF) molecule in USC with a quantized infrared electromagnetic field. We identify diabatic initial conditions of the coupled light–matter system that result in spontaneous molecular dissociation in the absence of external coherent or thermal infrared driving. The nonadiabatic nature of the state initialization is essential for the vacuum-assisted dissociation to occur, which is not expected for adiabatic state preparation.^{49,50} Using polaron transformation techniques, we gain analytical intuition into the role that the vibrational permanent dipole moments play in the proposed vacuum-assisted dissociation mechanism. The emergence of vibrational Bloch–Siegert (BS) shifts is predicted, in analogy with the QED phenomenology observed with Landau polaritons⁵¹ and superconducting qubits.⁴⁰ The ground-state Bloch–Siegert shift is shown to be a good predictor for the minimal light–matter coupling strength below which no spontaneous dissociation occurs.

Recent work in Ref. 52 predicted suppression of single-molecule dissociation relative to free space for far-detuned and near-resonant infrared cavities, by initializing the light–matter system in a specific initial diabatic state where the nuclear motion is above the bare dissociation energy and the cavity field has no

photons. By considering other choices of initial diabatic states that include diabatic states below the dissociation energy, we qualitatively confirm and further extend these findings by predicting the emergence of threshold behavior for dissociation with increasing coupling strength. Our results highlight the potential of ultrastrong light–matter interactions to enable novel ultrafast chemical reactivities at the single-molecule level in near-term nanophotonics experiments. Our predictions are valid for single-molecule systems for timescales shorter than molecular rotation, intramolecular energy redistribution, and characteristic photon loss timescales.

The article is organized as follows: In Sec. II, we review the MLQR model and the quantum dynamics method used to compute the dynamics of vibrational polariton wavepackets in the coordinate representation. In Sec. III, we introduce and characterize the initial product states of light and matter whose dissociation dynamics will be discussed. Section IV describes the ultrafast dissociation dynamics of each initial state, and in Sec. V, a polaron-frame analysis is introduced to gain analytical intuition into the process. Conclusions are given in Sec. VI.

II. MOLECULAR CAVITY QED

We model the reduced vibrational dynamics of a single HF molecule in an electromagnetic environment using multipolar cavity QED.^{21–25,53} The Hamiltonian of the system is given by ($\hbar \equiv 1$ is used throughout)

$$\hat{H} = \hat{T}(q) + \hat{T}(x) + \hat{V}_P(q, x), \quad (1)$$

where $\hat{T}(q)$ and $\hat{T}(x)$ are the molecular and photonic kinetic energy operators, respectively. The polariton potential energy surface,

$$\hat{V}_P(q, x) = \hat{V}(q) + \frac{1}{2} \omega_c^2 \hat{x}^2 + \sqrt{2\omega_c} \mathcal{E}_0 \hat{d}(q) \hat{x}, \quad (2)$$

includes the molecular $\hat{V}(q)$ potential energy curve, photonic harmonic oscillator potential, and dipolar interaction term. \hat{x} is the cavity field quadrature and $\hat{d}(q)$ is the electric dipole operator. Harmonic cavity photons have unit mass and resonance frequency ω_c . The electric field operator can be written as $\hat{E} = \sqrt{2\omega_c} \mathcal{E}_0 \hat{x}$. Vacuum fluctuations at the cavity frequency determine the field amplitude $\mathcal{E}_0 = \langle 0 | \hat{E}^2 | 0 \rangle^{1/2} \equiv \lambda_g \omega_{10} / d_{10}$. The dimensionless parameter λ_g is equal to the coupling ratio g/ω_c used in quantum optics,^{4,5,30} with $g = d_{10} \mathcal{E}_0$. ω_{10} and d_{10} are the fundamental vibration frequency and transition dipole moment, respectively. We ignore the rotational motion of molecules under the assumption that the rotational period is much longer (>10 ps) than the vibration–photon evolution timescales (~10–100 fs), so that the orientation of the vibrating dipole can be considered frozen over the relevant dissociation timescales. Improvements over this assumption can be found in Ref. 54.

Figure 1 shows the bare potential energy curve $V(q)$ and dipole moment function $d(q)$ of the HF molecule in the ground electronic state $X^1\Sigma^+$, computed using a complete active space in the multi-configuration self-consistent field level. The multireference configuration interaction (MRCI) method is employed using Dunning's correlation-consistent basis set with diffuse functions aug-cc-pVQZ. All electronic structure calculations were carried out

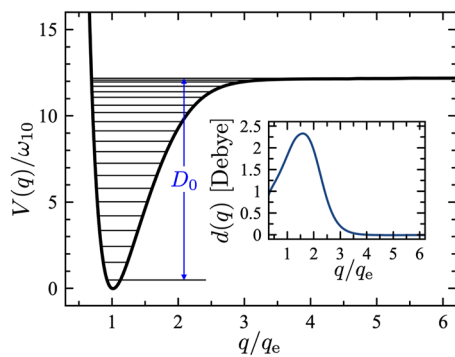


FIG. 1. *Ab initio* potential energy curve $\hat{V}(q)$ of the electronic ground state $X^1\Sigma^+$ for the HF molecule. The bond length q is in units of the equilibrium distance $q_e = 0.91 \text{ \AA}$. Horizontal lines represent the 22 vibrational bound states, and $D_0 = 12.16\omega_{10}$ is the dissociation energy. Inset: electric dipole moment function $d(q)$ along the scaled bond distance.

using the software MOLPRO.⁵⁵ Following the nomenclature from Ref. 7, the dipole function of HF corresponds to a polar-right species, that is, the vibrational mode has a finite dipole moment with a positive slope at equilibrium. Other diatomic molecules of the same class include LiH,³⁶ LiF,⁵⁶ and NaI.⁵⁷

To propagate the vibrational polariton wave function in coordinate space, we solve the time-dependent Schrödinger equation with the Hamiltonian in Eq. (1), using the multi-configuration time-dependent Hartree (MCTDH) method.^{58–60} MCTDH was primarily developed to describe non-adiabatic photochemistry of polyatomic molecules^{61–63} and has recently been adapted to study cavity chemistry.^{7,54,64–67} Recent extensions of the MCTDH method have been developed for treating strongly interacting quantum oscillators with Markovian dissipation.⁶⁸

The MCTDH wavefunction ansatz for molecular and photonic degrees of freedom is given by

$$\Psi(q, x, t) = \sum_{j_q=1}^{n_q} \sum_{j_x=1}^{n_x} A_{j_q j_x}(t) \phi_{j_q}(q, t) \phi_{j_x}(x, t), \quad (3)$$

which is a product expansion of time-dependent basis functions $\phi_{j_q}(q, t)$ and $\phi_{j_x}(x, t)$ weighted by time-dependent coefficients $A_{j_q j_x}$. To compute photonic and vibrational observables, we project the time-dependent light-matter wavefunction $\Psi(q, x, t)$ in a vibrational or photonic subspace to obtain expectation values of molecular or field operators.

Calculations are performed using a DVR-sine primitive basis set for the vibrational coordinate q and a DVR-HO basis set for the displacement operator of the photonic mode x . Results are obtained by setting the molecular and photonic coordinates in boxes of $N_q = 681$ grid points on the interval $0.4 < q < 14.0$ bohr and $N_x = 451$ grid points between the dimensionless interval $-100 < x < 100$, respectively. These parameters capture the 22 vibrational bound states of the HF potential, as well as a converged number of free scattering states with box normalization. The computed fundamental transition frequency of HF is $\omega_{10} = 3989 \text{ cm}^{-1}$, which agrees with experiments.⁶⁹ The number of single-particle functions used is in the interval $n_q, n_x = [30, 70]$. Each value is suitably chosen to

numerically converge the wave packet propagation at a given value of λ_g and detuning $\Delta = \omega_c - \omega_{10}$.

III. DIABATIC INITIAL STATES

The state preparation strategy commonly used in experiments is thermal equilibration of light-matter states with their reservoir.⁷⁰ As discussed below, this approach does not lead to spontaneous bond dissociation. Recently, an alternative state preparation to produce vibration-photon diabatic states using ultrafast photochemistry was proposed.⁷ The protocol consists of locating a single molecule within a plasmonic mode volume, followed by an external pulse that suddenly activates the light-matter coupling in a time interval Δt smaller than the Rabi period, creating a diabatic state that is a superposition of polariton eigenstates. On the contrary, if Δt is larger than the Rabi period, that is, thermal equilibration, the coupled system evolves adiabatically to a polariton eigenstate. Similarly, schemes of ultrafast preparation of nonthermal vibrational energy distributions have been demonstrated in photoisomerization using pump-probe experiments.⁷¹ For state preparation steps that are much faster than the thermal equilibration timescales ($\sim 1 - 10$ ps), it is possible to produce excited vibrational polariton wavepackets beyond the usually accessed lower and upper polariton.

Here, we discuss the dissociation dynamics of different vibration-photon states that are initially in the product form

$$\Psi(q, x) = N \phi(q) \varphi(x) = N e^{-\frac{(q-\langle q \rangle)^2}{4(\Delta q)^2}} e^{-\frac{(x-\langle x \rangle)^2}{4(\Delta x)^2}}, \quad (4)$$

where $\phi(q)$ is a Gaussian function in the molecular coordinate q and $\varphi(x)$ a Gaussian in the photonic coordinate x . The initial Gaussian wavepackets in the (q, x) -space are centered at $\langle \hat{q} \rangle$ and $\langle \hat{x} \rangle$, with variances $\langle \Delta \hat{q} \rangle^2 = \langle \hat{q}^2 \rangle - \langle \hat{q} \rangle^2$ and $\langle \Delta \hat{x} \rangle^2 = \langle \hat{x}^2 \rangle - \langle \hat{x} \rangle^2$. The first and second moments define the initial mean energy of the light-matter state $\langle E \rangle = \langle \hat{H} \rangle$ and its energy variance $\langle \Delta E \rangle^2 = \langle \hat{H}^2 \rangle - \langle \hat{H} \rangle^2$, with \hat{H} from Eq. (1). N is a normalization factor. Table I shows the position and broadening (standard deviation) parameters in configuration space for four initial states denoted $|\Psi_A\rangle$, $|\Psi_B\rangle$, $|\Psi_C\rangle$, and $|\Psi_D\rangle$, which are described below. The parameters of the polariton ground state $|\Psi_{GS}\rangle$ at $\lambda_g = 0.2$ are also given.

The wavefunction in Eq. (4) can also be written in the uncoupled vibration-photon basis as

$$|\Psi\rangle = \sum_v C_v |v\rangle \otimes \sum_n P_n |n\rangle, \quad (5)$$

TABLE I. Location and spread in configuration space of the initial diabatic states. The parameters of the coupled ground state (GS) for $\lambda_g = 0.2$ and $\Delta = 0$ are also given. Molecular lengths are in units of $q_e = 0.91 \text{ \AA}$.

State	$\langle \hat{q} \rangle/q_e$	$\langle \hat{x} \rangle$	$\langle \Delta \hat{q} \rangle/q_e$	$\langle \Delta \hat{x} \rangle$
$ \Psi_A\rangle$	1.30	-16.5	0.23	5.25
$ \Psi_B\rangle$	1.5	-8.5	0.23	5.25
$ \Psi_C\rangle$	1.0	0.0	0.13	5.25
$ \Psi_D\rangle$	1.0	7.2	0.13	6.49
$ \Psi_{GS}\rangle$	1.36	-45.9	0.14	5.31

where $C_v = \langle v | \phi(q) \rangle$ and $P_n = \langle n | \phi(x) \rangle$ are the expansion coefficients for bare molecular and photonic wavepackets, respectively. $|v\rangle$ is a vibrational eigenstate with quantum number v , and $|n\rangle$ is a cavity Fock state with n photons. Diabatic states of product form have been considered for intracavity dynamics in Refs. 7 and 52.

Figure 2 characterizes the energy content of the initial product states in two complementary ways. Figure 2(a) illustrates the center position and spread of each initial state on the polaritonic energy surface $\hat{V}_P(q, x)$ of HF inside a cavity with $\lambda_g = 0.20$ and zero detuning ($\omega_c = \omega_{10}$). The polariton ground state $|\Psi_{GS}\rangle$ has a well-defined location at the bottom of the potential energy surface with $\langle \hat{q} \rangle_{GS} \approx 1.4q_e$ and $\langle \hat{x} \rangle_{GS} \approx -46$. The equilibrium distance of the polariton ground state is shifted along the molecular coordinate closer to the position where the dipole moment is maximum ($q \sim 1.4q_e$) due to the contribution of the interaction term $\hat{d} \cdot \hat{E}$ to the polariton potential energy surface. This bond-softening effect was first studied in Ref. 7. Since the potential $V_P(q, x)$ does not have long-range barriers, initial product states that are high enough in the potential have the possibility of moving and spreading in configuration space toward the large q region, where bond dissociation occurs.

Figures 2(b)–2(e) show the probability distribution of the initial states $|\Psi_A\rangle$ to $|\Psi_D\rangle$, respectively, in the polariton eigenbasis $|\epsilon\rangle$, in which Eq. (1) is diagonal. State $|\Psi_A\rangle$ has the lowest

mean energy $\langle E \rangle_A = -11.0\omega_{10}$, relative to the free-space ground state $|v = 0\rangle |n = 0\rangle$. The energy spreading of the state is $\langle \Delta E \rangle_A \approx 7.5\omega_{10}$, which, as Fig. 2(b) shows, involves polariton components whose energies are below the equivalent of the free-space dissociation energy D_0 (blue dashed line), relative to the coupled ground state energy $E_{GS} = -16.45\omega_{10}$. This is consistent with the location of the wavepacket in coordinate space in Fig. 2(a), which is above the ground state but below the dissociation contour defined by $V_P = D_0$.

The mean energy of state $|\Psi_B\rangle$ is $\langle E \rangle_B = -7.0\omega_{10}$, which is higher than $|\Psi_A\rangle$, and its energy spread $\langle \Delta E \rangle \approx 6.4\omega_{10}$ is such that a significant fraction of the wavepacket has energy components above D_0 , as Fig. 2(c) shows. Again, this is expected from the location and spread of the state in the potential energy surface [Fig. 2(a)]. States $|\Psi_A\rangle$ and $|\Psi_B\rangle$ can be seen as excited polaritonic wave packets with mean energies above the lowest polariton eigenstates (LP and UP) and below the bare dissociation energy ($E_{UP} < \langle \hat{H} \rangle < D_0$).

The other two initial states studied are the bare ground state $|\Psi_C\rangle \equiv |v = 0\rangle |n = 0\rangle$, and an excited variant of this where the molecule has no vibrational excitations but the cavity field has a finite number of thermal photons, that is, $|\Psi_D\rangle \equiv |v = 0\rangle \otimes \sum_n P_n |n\rangle$. State $|\Psi_C\rangle$ is at the uncoupled equilibrium coordinates $\langle \hat{q} \rangle = q_e$ and $\langle \hat{x} \rangle = 0.0$ in Fig. 2(a), which are high in the potential energy surface relative to the polariton ground state. The energy distribution in Fig. 2(d) shows that the state is centered at the

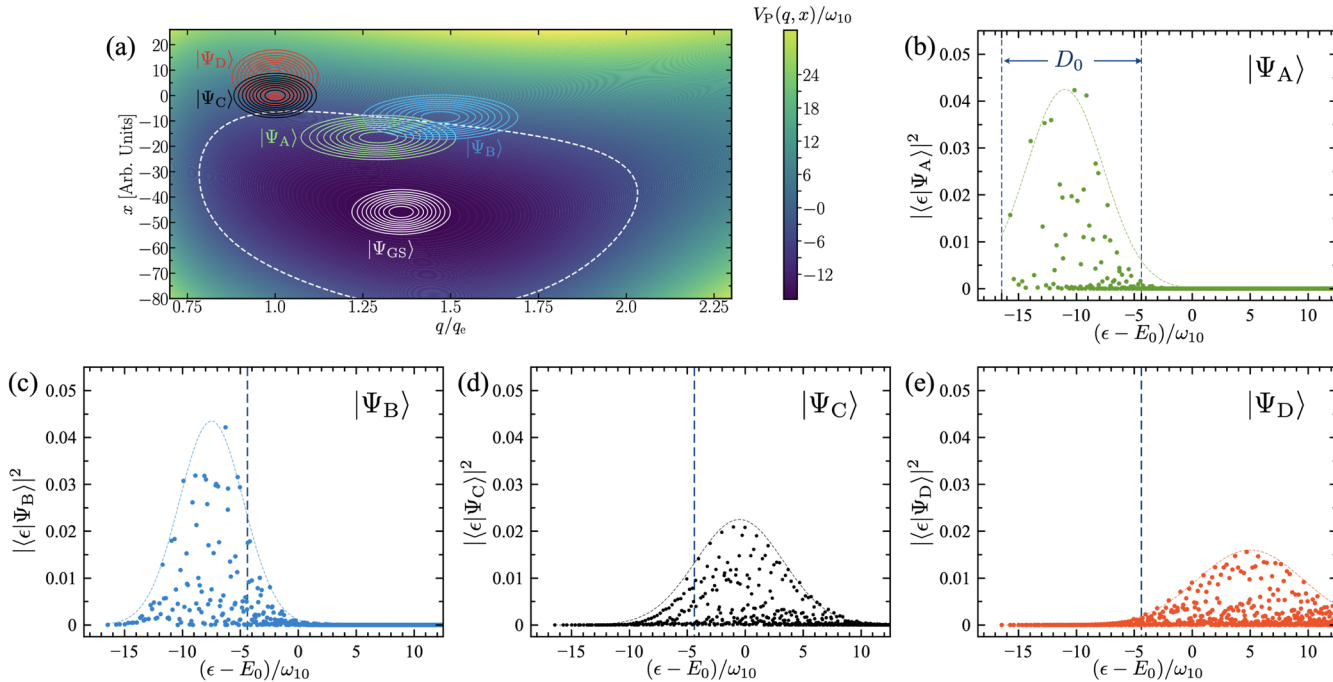


FIG. 2. (a) Polariton potential energy surface $V_P(q, x)$ with contour lines showing the distribution of the initial wavepackets $|\Psi_A\rangle$, $|\Psi_B\rangle$, $|\Psi_C\rangle$, and $|\Psi_D\rangle$. The polariton ground state $|\Psi_{GS}\rangle$ is shown for reference. The dashed white contour corresponds to $V_P = D_0$. (b) Probability distribution of the initial wavepacket $|\Psi_A\rangle$ in the polariton eigenbasis $|\epsilon\rangle$, as a function of the energy difference with respect to the bare ground state energy E_0 , in units of the fundamental vibration frequency ω_{10} . The dashed line is a guide to the eye. (c) Energy distribution of state $|\Psi_B\rangle$. (d) Energy distribution of state $|\Psi_C\rangle = |0\rangle|0\rangle$. (e) Energy distribution of state $|\Psi_D\rangle$. In each panel, the vertical dashed blue line marks the bare dissociation energy D_0 with respect to polariton ground state. The coupling strength parameter is $\lambda_g = 0.20$ and the detuning $\Delta = 0$.

uncoupled ground state energy $\langle E \rangle = 0$ and contains a significant number of components above D_0 . This means that higher dissociation probabilities can be expected in comparison with states $|\Psi_A\rangle$ and $|\Psi_B\rangle$.

By assuming an initial thermal excitation of the cavity field with $\bar{n} = 0.58$ average photons, state $|\Psi_D\rangle$ is displaced vertically in configuration space relative to $|\Psi_C\rangle$ in Fig. 2(a). This corresponds to a displacement and broadening of the wavepacket in the polariton energy basis toward higher energies. Figure 2(e) shows that most of the energy components of state $|\Psi_D\rangle$ are above D_0 , so the highest dissociation probabilities can be expected during free evolution, as confirmed below. Initial thermal excitations of the photon field could be expected in diabatic state preparation strategies based on photochemistry,⁷ which focus on preparing nonequilibrium vibrational states over times much faster than the Rabi interaction.

IV. FREE DISSOCIATION DYNAMICS

Having established the relevant properties of the initial light-matter product states $|\Psi(0)\rangle$, we now study the free evolution of each initial state with the propagator $U(t) = \exp[-i\hat{H}t]$, with \hat{H} given by Eq. (1). Wavepacket propagation is carried out in coordinate space with the MCTDH method, as described in Sec. II.

At each time step, we evaluate the bond dissociation probability $P_{\text{diss}}(t)$, which we define for vibrational polariton wavepackets $|\Psi(t)\rangle$ in terms of the projected population into bare bound vibrational states $|\nu\rangle$ as

$$P_{\text{diss}}(t) = 1 - \sum_{\nu=0}^{N_b} |\langle \nu | \Psi(t) \rangle|^2, \quad (6)$$

where N_b is the vibrational quantum number of the highest-energy bound state supported by the bare molecular potential energy curve $V(q)$. For HF, we have $N_b = 21$. Equation (6) implicitly includes a trace over the photonic components of $|\Psi\rangle$. The instantaneous mean bond length $\langle \hat{q}(t) \rangle$ and the bond spreading $\langle \Delta \hat{q}(t) \rangle$ are also monitored.

Figure 3(a) shows the evolution of the HF bond length $\langle \hat{q} \rangle$ for the four initial states described above, in a resonant cavity ($\Delta = 0$) with coupling strength $\lambda_g = 0.2$. The results show that after a few vibrational periods (~ 10 fs), vibrational ladder climbing stops and stabilizes, giving mean bond lengths equivalent to excited bare vibrational levels $\nu = 8-12$. Bond lengthening as witnessed by $\langle \hat{q} \rangle$ was first discussed in Ref. 7 for vibrational polaritons. The largest bond length $\langle \hat{q} \rangle \approx 1.6q_e$ (equivalent to $\nu = 12$) is reached for the initial state $|\Psi_D\rangle$, due to its initially excited photonic content. Interestingly, although state $|\Psi_B\rangle$ is initially farther from equilibrium distance q_e than the bare ground state $|\Psi_C\rangle$ ($|0\rangle|0\rangle$), upon free evolution with the infrared vacuum the two polariton wavepackets tend to stabilize around $\langle \hat{q} \rangle \approx 1.45q_e$ in about 100 fs.

Figure 3(b) shows the corresponding evolution of broadening in q -space. For all states, the value of $\langle \Delta \hat{q} \rangle$ tends to stabilize less quickly than the mean value $\langle \hat{q} \rangle$, but after a few hundred femtoseconds, the wavepacket stops spreading and undergoes coherent breathing dynamics in q -space. This breathing dynamics is more evident for state $|\Psi_D\rangle$, which shows the largest spreading of all states. Interestingly, although states $|\Psi_B\rangle$ and $|\Psi_C\rangle$ both stabilize with essentially the same bond length $\langle \hat{q} \rangle$, the bond spreading of $|\Psi_C\rangle$ is about 70% higher than $|\Psi_B\rangle$ at 200 fs.

Figure 3(c) shows the evolution of P_{diss} corresponding to panels 3(a) and 3(b). After stabilization is established, the dissociation probability reaches $\approx 20\%-30\%$ for states $|\Psi_C\rangle$ and $|\Psi_D\rangle$, the latter having a slightly higher dissociation rate. For comparison, dissociation probabilities of this magnitude could be reached for gas-phase HF molecules in free space with a resonant monochromatic laser of intensity on the order of 10^{14} W/cm^2 . This highlights how efficiently the infrared vacuum can assist the vibrational ladder-climbing process in a nanocavity. The long-time dissociation probabilities of states $|\Psi_A\rangle$ and $|\Psi_B\rangle$ are one and three orders of magnitude smaller, respectively, than states $|\Psi_B\rangle$ and $|\Psi_C\rangle$. This behavior correlates with the relative weights in the distribution of excited polariton components whose energy exceeds D_0 above the coupled ground state GS in Figs. 2(b)–2(e).

Figure 4 shows the joint dependence of the long-time dissociation probability (P_{diss} at $t = 200$ fs) with detuning Δ and

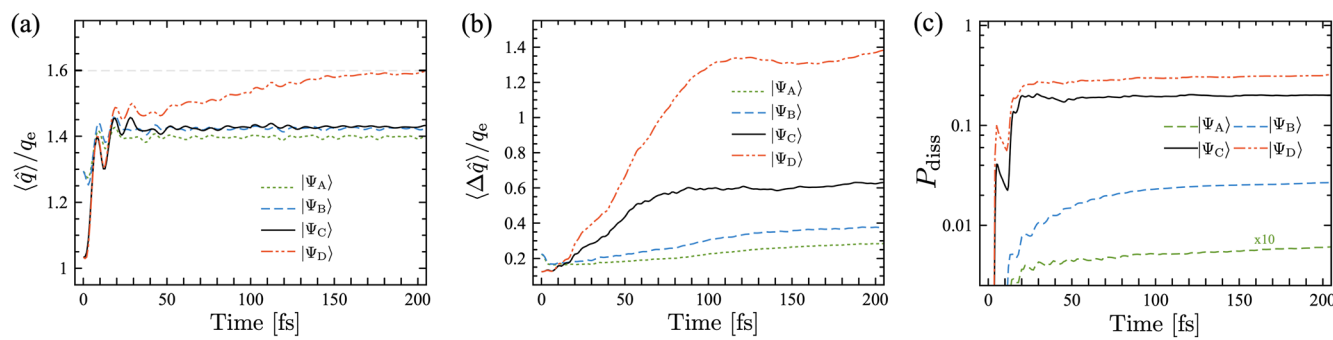


FIG. 3. (a) Mean bond length $\langle \hat{q} \rangle$, in units of q_e , as a function of time for different initial diabatic states. (b) Bond length standard deviation $\langle \Delta \hat{q} \rangle$ for the same states. (c) Dissociation probability P_{diss} as a function of time. The molecular vibration is on exact resonance with a cavity mode ($\omega_c = \omega_{10}$) in ultrastrong coupling ($\lambda_g = 0.20$). $q_e = 0.91 \text{ \AA}$ is the equilibrium bond length of HF in free space.

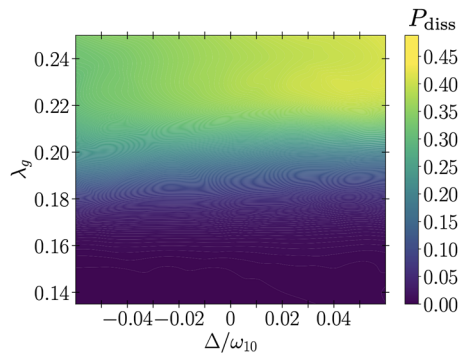


FIG. 4. Dissociation probability P_{diss} as a function of cavity detuning Δ/ω_{10} and Rabi coupling strength λ_g at $t = 200$ fs, for a single-mode cavity initialized in the bare vacuum initial diabatic state $|\Psi_C\rangle$.

coupling strength λ_g , for state $|\Psi_C\rangle$. Although the cavity frequency dependence is weak for all the coupling strengths considered, blue-detuned cavities consistently tend to give slightly higher values of P_{diss} than red-detuned cavities, which we attribute to an increasing energy content of the initial state with cavity frequency. For a given cavity frequency, the dissociation probability grows rapidly from zero up to a saturation value after a threshold coupling is passed. For $\Delta = 0$, the threshold for spontaneous dissociation is $\lambda_g \approx 0.17$ for $|\Psi_C\rangle$. Saturation is reached when all the unbound components of the polariton wavepacket have decayed via dissociation and only bound contributions remain. Similar trends are found for the other initial states.

V. ORIGIN OF THE COUPLING THRESHOLD FOR SPONTANEOUS DISSOCIATION

In this section, we aim to understand the origin of the threshold coupling strength λ_g seen in Fig. 4, for the spontaneous dissociation of state $|\Psi_C\rangle = |0\rangle|0\rangle$. Since this is also the ground state of the uncoupled system ($\lambda_g = 0$), we can fully characterize its behavior with increasing coupling strength using polaron transformation techniques, following ideas used for studying light-matter coupling in circuit QED.^{72–75}

By projecting the system Hamiltonian in Eq. (1) to the bare vibrational energy basis $|\nu\rangle$, with the field quadrature written as $\sqrt{2\omega_c}\hat{x} = \hat{a}^\dagger + \hat{a}$, where \hat{a} is the field annihilation operator, the system Hamiltonian can be rewritten as $\hat{H} = \hat{H}_0 + \hat{H}_1$, with⁷

$$\hat{H}_0 = \omega_c \hat{a}^\dagger \hat{a} + \sum_{\nu} \omega_{\nu} |\nu\rangle\langle\nu| + \mathcal{E}_0 \sum_{\nu} d_{\nu\nu} |\nu\rangle\langle\nu| \otimes (\hat{a} + \hat{a}^\dagger), \quad (7)$$

and

$$\hat{H}_1 = \mathcal{E}_0 \sum_{\nu} \sum_{\nu' \neq \nu} d_{\nu'\nu} |\nu'\rangle\langle\nu| \otimes (\hat{a} + \hat{a}^\dagger), \quad (8)$$

where $d_{\nu\nu} = \langle\nu|d(q)|\nu\rangle \geq 0$ is the vibrationally averaged permanent dipole moment of the ν -th state and $d_{\nu'\nu} = \langle\nu'|d(q)|\nu\rangle$ is a transition dipole moment between states $|\nu'\rangle$ and $|\nu\rangle$. Figure 5(a) shows the permanent and transition dipoles of HF as a function of quantum number ν , with transition dipoles starting from $\nu = 0$ and $\nu = 1$. Permanent dipoles are larger than the transition dipoles by an order of

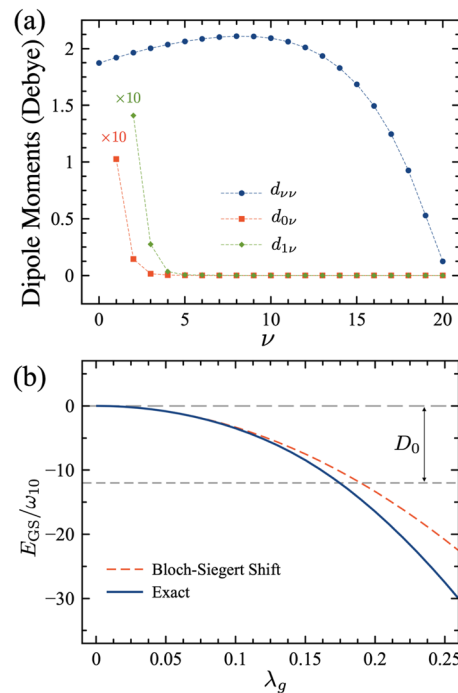


FIG. 5. (a) Permanent ($d_{\nu\nu}$) and transition ($d_{\nu'\nu}$) dipole moments as a function of the vibrational quantum number ν for HF molecules. Transition dipoles are multiplied by a factor of 10. (b) Bloch-Siegert shift and polariton ground state energy E_{GS} , in units of ω_{10} , as a function of coupling strength λ_g . The gray dashed lines mark the equivalent of the free-space dissociation energy D_0 .

magnitude, both for fundamental transitions ($\Delta\nu = \pm 1$) and overtones ($|\Delta\nu| \geq 2$). State-dependent Rabi couplings can be defined as $g_{\nu'\nu} = d_{\nu'\nu} \mathcal{E}_0$. The generalization of Eqs. (7) and (8) to many molecules is straightforward.^{76–78}

We now rewrite the system Hamiltonian in the polaron frame as $\tilde{\mathcal{H}} \equiv \hat{D}\hat{H}\hat{D}^\dagger = \tilde{\mathcal{H}}_0 + \tilde{\mathcal{H}}_1$,^{74,79} using the unitary polaron transformation,

$$\hat{D}(\lambda_p) = \exp \left[\lambda_p \sum_{\nu} (d_{\nu\nu}/d_{10}) |\nu\rangle\langle\nu| \otimes (\hat{a}^\dagger - \hat{a}) \right], \quad (9)$$

with dimensionless displacement $\lambda_p \equiv \lambda_g \omega_{10}/\omega_c$. Diagonal dipole matrix elements are scaled by the fundamental transition dipole d_{10} . In this polaron frame, \hat{H}_0 becomes diagonal in the uncoupled Fock basis and is given by

$$\tilde{\mathcal{H}}_0 \equiv \hat{D}\hat{H}_0\hat{D}^\dagger = \sum_{\nu} (\omega_{\nu} - \eta_{\nu}) |\nu\rangle\langle\nu| + \omega_c \hat{a}^\dagger \hat{a}, \quad (10)$$

where $\eta_{\nu} = \lambda_p^2 \omega_c (d_{\nu\nu}/d_{10})^2$ is the Bloch-Siegert shift of the ν -th vibrational level. These vacuum-induced *red shifts* have been measured for superconducting qubits⁴⁰ and Landau polaritons.⁵¹ On the contrary, material levels are *blue-shifted* by the vacuum in the Pauli-Fierz model.⁴⁸

The polaron-transformed Rabi coupling term $\tilde{\mathcal{H}}_1$ now reads

$$\tilde{\mathcal{H}}_1 = \mathcal{E}_0 \sum_v \sum_{v' \neq v} \tilde{d}_{v'v} |v'\rangle \langle v| e^{\lambda_p \Delta d_{v'v} (\hat{a}^\dagger - \hat{a})} (\hat{a} + \hat{a}^\dagger), \quad (11)$$

where $\tilde{d}_{v'v} \equiv d_{v'v} (1 - 2\lambda_p d_{vv}/d_{10})$ is a renormalized coupling strength, with $\Delta d_{v'v} \equiv (d_{v'v} - d_{vv})/d_{10}$ being the scaled difference of permanent dipole moments between vibrational states $|v\rangle$ and $|v'\rangle$. Equation (11) shows that strongly polar vibrational states ($d_{vv} \gg d_{10}$) should experience a reduced coupling with the cavity field relative to non-polar vibrations for equal vacuum field confinements (\mathcal{E}_0). For molecules whose permanent dipoles exhibit strong variations across the vibrational spectrum, multi-photon interaction processes driven by the exponential term in Eq. (11) should become efficient at short times. Without permanent dipoles ($d_{vv} \sim 0$), the polaron frame Hamiltonian $\tilde{\mathcal{H}}$ reduces to the multi-level quantum Rabi (MLQR) model.⁶

For polar vibrations in USC (e.g., HF, CO, H₂O), the vibrational polariton ground state (GS) is very different from the diabatic ground state $|v=0\rangle|n=0\rangle$ (state $|\Psi_C\rangle$). The polariton ground state is a superposition of uncoupled states $|v\rangle|n\rangle$ with potentially high quantum numbers v and n , depending on the value of λ_g .^{7,66} The Bloch–Siegert shift of the polariton ground state relative to the uncoupled ground level is obtained directly from Eq. (10) for $v=0$ to give

$$E_{\text{BS}} = -d_{00}^2 \mathcal{E}_0^2 / \omega_c. \quad (12)$$

As Fig. 5(b) shows, the Bloch–Siegert shift is a good approximation for the ground-state energy in strong coupling $\lambda_g \ll 0.1$ ($\Delta = 0$), but underestimates the contributions of avoided crossings and counter-rotating wave interactions that $\tilde{\mathcal{H}}_1$ introduce. By comparing E_{BS} with the bare dissociation energy D_0 , one can estimate the threshold coupling parameter λ_g beyond which the initial state $|\Psi_C\rangle$ could spontaneously dissociate upon free evolution. For an HF molecule in a resonant cavity, Eq. (12) gives $E_{\text{BS}} = D_0$ for $\lambda_g \approx 0.18$, which agrees well with the threshold obtained via wavepacket propagation in Fig. 4.

The existence of a threshold coupling for spontaneous dissociation is a statement about the relative energy content of the initial light–matter wavepacket. As such, it could be generalized by establishing as a necessary condition that the mean energy of the initial state, $\langle \hat{H} \rangle_0$, relative to the ground polariton energy level, should be at least equal to the bare molecular dissociation energy, that is,

$$\langle \hat{H}(\lambda_g) \rangle_0 - E_{\text{GS}}(\lambda_g) \geq D_0, \quad (13)$$

where the coupling-strength dependence of the left-hand side is made explicit. For $|\Psi_C\rangle$, we have $\langle \hat{H} \rangle_0 = 0$, and Eq. (13) gives the threshold coupling found above ($\lambda_g = 0.18$), when E_{GS} is approximated by Eq. (12). We expect this coupling threshold condition to hold not only for diatomic polar molecules but also for high-frequency polar anharmonic vibrations of polyatomic molecules that only couple weakly to other intramolecular vibrational modes.

Figure 6(a) shows the energy functional $F \equiv \langle \hat{H} \rangle_0 - E_{\text{GS}} - D_0$ as a function of coupling strength λ_g for the same diabatic initial states used in Fig. 3. The polariton ground state energy E_{GS} is calculated

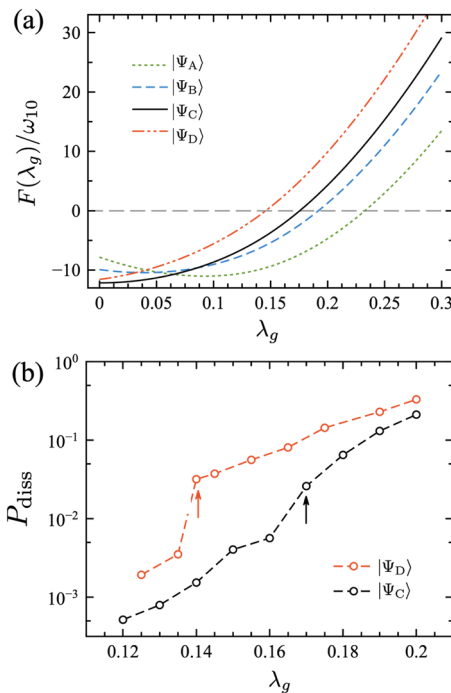


FIG. 6. (a) Relative energy functional $F(\lambda_g) \equiv \langle \hat{H}(\lambda_g) \rangle_0 - E_{\text{GS}}(\lambda_g) - D_0$ as a function of coupling strength λ_g for different initial diabatic states. (b) Long-time dissociation probability P_{diss} (at 200 fs) as a function of coupling strength λ_g for an HF molecule on a resonant cavity ($\omega_c = \omega_{10}$), for the initial diabatic states $|\Psi_C\rangle$ and $|\Psi_D\rangle$. Arrows mark the onset of spontaneous dissociation.

by diagonalizing Eq. (1), and the mean energy $\langle \hat{H} \rangle_0$ is obtained from the ansatz in Eq. (4). From the condition in Eq. (13), the function $F(\lambda_g)$ changes sign from negative to positive when the initial state has sufficient energy for spontaneous dissociation. Complementing the results in Fig. 3, which were obtained at fixed $\lambda_g = 0.2$, Fig. 6(a) shows that threshold couplings are higher for the states with lower initial energy content, with states $|\Psi_C\rangle$ and $|\Psi_D\rangle$ having the smallest thresholds.

In Fig. 6(b), we compare the predicted thresholds based on the condition $F(\lambda_g) = 0$ for states $|\Psi_C\rangle$ ($\lambda_g = 0.175$) and $|\Psi_D\rangle$ ($\lambda_g = 0.145$), with those obtained by propagating the states as in Fig. 3(c), for different values of λ_g . The computed long-time dissociation probabilities $P_{\text{diss}} (t \approx 200 \text{ fs})$ confirm the existence of a threshold for state $|\Psi_C\rangle$ near $\lambda_g \approx 0.170$ and for state $|\Psi_D\rangle$ near $\lambda_g \approx 0.140$, which compare well with the threshold estimates based on Eq. (13). We confirmed that states $|\Psi_A\rangle$ and $|\Psi_B\rangle$ also show threshold behavior at higher couplings.

VI. CONCLUSIONS

We have studied a previously unexplored mechanism for spontaneously dissociating a single molecule in the presence of strongly confined infrared vacuum, with high efficiency over sub-picosecond timescales. Dissociation occurs due to ultrastrong coupling of the vibrational motion with the vacuum field in the absence of other coherent and incoherent energy sources and cannot be properly

understood in terms of classical motion on a polaritonic potential energy surface because it is driven by wavepacket broadening in phase space. This lack of immediate classical analog highlights the coherent quantum mechanical nature of the reactive process.

Through a combined numerical and analytical analysis, we showed that spontaneous dissociation requires a threshold light-matter coupling strength to occur and the ability to prepare the system in a diabatic wavepacket with sufficient excitation content over timescales much faster than thermalization. Our numerical results were based on hydrogen fluoride as a case study but general universal conditions are established for assessing the feasibility of achieving spontaneous dissociation for an arbitrary molecule [Eq. (13)]. These findings are valid for systems with photonic and material relaxation times much longer than the sub-picosecond ladder climbing and dissociation timescales. The photon lifetime in infrared nanoresonators varies in the range 10^2 – 10^3 fs,⁸⁰ setting the limits of the quantitative validity of our predictions. The analysis of intracavity dissociation in the presence of ultrafast photon loss in ultrastrong coupling requires a consistent derivation of a quantum master equation⁸¹ that can be integrated numerically using existing methodologies.^{67,68} This is the subject of future work.

Techniques for implementing ultrafast light-matter state preparation are currently available,⁷ but reaching ultrastrong coupling with individual molecular vibrations in infrared nanocavities is still an open problem. However, recent works have demonstrated the ability to engineer the electromagnetic vacuum in nanoscale gaps with infrared resonances,^{20,82} including ultrastrong coupling to material vibrational resonances,⁸³ which could enable the study of coherent vacuum-assisted chemical processes at the single-molecule level in the near future, and our work establishes basic physical principles for such a new regime of chemical reactivity.

ACKNOWLEDGMENTS

We thank Adrián E. Rubio López, Johannes Schachenmayer, and Blake S. Simpkins for comments. J.F.T. is supported by ANID-Fondecyt Iniciación Grant No. 11230679. F.H. is supported by ANID-Fondecyt Regular Grant No. 1221420 and the Air Force Office of Scientific Research under Award No. FA9550-22-1-0245. The authors also thank support from the ANID-Millennium Science Initiative Program No. ICN17_012.

AUTHOR DECLARATIONS

Conflict of Interest

The authors have no conflicts to disclose.

Author Contributions

Johan F. Triana: Conceptualization (equal); Formal analysis (equal); Methodology (equal); Software (lead); Supervision (equal); Validation (lead); Writing – original draft (lead). **Felipe Herrera:** Conceptualization (equal); Formal analysis (equal); Methodology (equal); Supervision (equal); Writing – review & editing (lead).

DATA AVAILABILITY

The data that support the findings of this study are available within the article.

REFERENCES

- 1 C. L. Degen, F. Reinhard, and P. Cappellaro, *Rev. Mod. Phys.* **89**, 035002 (2017).
- 2 G. Wendum, *Rep. Prog. Phys.* **80**, 106001 (2017).
- 3 A. J. Shields, *Nat. Photonics* **1**, 215 (2007).
- 4 P. Forn-Díaz, L. Lamata, E. Rico, J. Kono, and E. Solano, *Rev. Mod. Phys.* **91**, 025005 (2019).
- 5 A. Frisk Kockum, A. Miranowicz, S. De Liberato, S. Savasta, and F. Nori, *Nat. Rev. Phys.* **1**, 19 (2019).
- 6 F. J. Hernández and F. Herrera, *J. Chem. Phys.* **151**, 144116 (2019).
- 7 J. F. Triana, F. J. Hernández, and F. Herrera, *J. Chem. Phys.* **152**, 234111 (2020).
- 8 A. A. Anappara, S. De Liberato, A. Tredicucci, C. Ciuti, G. Biasiol, L. Sorba, and F. Beltram, *Phys. Rev. B* **79**, 201303 (2009).
- 9 T. Niemczyk, F. Deppe, H. Huebl, E. P. Menzel, F. Hocke, M. J. Schwarz, J. J. Garcia-Ripoll, D. Zueco, T. Hümmer, E. Solano, A. Marx, and R. Gross, *Nat. Phys.* **6**, 772 (2010).
- 10 M. Mazzeo, A. Genco, S. Gambino, D. Ballarini, F. Mangione, O. Di Stefano, S. Patanè, S. Savasta, D. Sanvitto, and G. Gigli, *Appl. Phys. Lett.* **104**, 233303 (2014).
- 11 J. George, T. Chervy, A. Shalabney, E. Devaux, H. Hiura, C. Genet, and T. W. Ebbesen, *Phys. Rev. Lett.* **117**, 153601 (2016).
- 12 F. Barachati, J. Simon, Y. A. Getmanenko, S. Barlow, S. R. Marder, and S. Kéna-Cohen, *ACS Photonics* **5**, 119 (2018).
- 13 R. Chikkaraddy, V. A. Turek, N. Kongswan, F. Benz, C. Carnegie, T. van de Goor, B. de Nijs, A. Demetriadou, O. Hess, U. F. Keyser, and J. J. Baumberg, *Nano Lett.* **18**, 405 (2018).
- 14 D. Wang, H. Kelkar, D. Martin-Cano, D. Rattenbacher, A. Shkarin, T. Utikal, S. Götzinger, and V. Sandoghdar, *Nat. Phys.* **15**, 483 (2019).
- 15 O. S. Ojambati, R. Chikkaraddy, W. D. Deacon, M. Horton, D. Kos, V. A. Turek, U. F. Keyser, and J. J. Baumberg, *Nat. Commun.* **10**, 1049 (2019).
- 16 M. Kuisma, B. Rousseaux, K. M. Czajkowski, T. P. Rossi, T. Shegai, P. Erhart, and T. J. Antosiewicz, *ACS Photonics* **9**, 1065 (2022).
- 17 D. A. Bandurin, D. Svitsov, I. Gayduchenko, S. G. Xu, A. Principi, M. Moshkin, I. Tretyakov, D. Yagodkin, S. Zhukov, T. Taniguchi, K. Watanabe, I. V. Grigorieva, M. Polini, G. N. Goltsman, A. K. Geim, and G. Fedorov, *Nat. Commun.* **9**, 5392 (2018).
- 18 B. Yao, Y. Liu, S.-W. Huang, C. Choi, Z. Xie, J. Flor Flores, Y. Wu, M. Yu, D.-L. Kwong, Y. Huang, Y. Rao, X. Duan, and C. W. Wong, *Nat. Photonics* **12**, 22 (2018).
- 19 A. B. Grafton, A. D. Dunkelberger, B. S. Simpkins, J. F. Triana, F. J. Hernández, F. Herrera, and J. C. Owrutsky, *Nat. Commun.* **12**, 214 (2021).
- 20 R. Wilcken, J. Nishida, J. F. Triana, A. John-Herpin, H. Altug, S. Sharma, F. Herrera, and M. B. Raschke, *Proc. Natl. Acad. Sci.* **120**, e2220852120 (2023).
- 21 E. A. Power, S. Zienau, and H. S. W. Massey, *Philos. Trans. R. Soc. London, Ser. A* **251**, 427 (1959).
- 22 P. W. Atkins, R. G. Woolley, and C. A. Coulson, *Proc. R. Soc. London, Ser. A* **319**, 549 (1970).
- 23 R. G. Woolley and C. A. Coulson, *Proc. R. Soc. London, Ser. A* **321**, 557 (1971).
- 24 E. A. Power and T. Thirunamachandran, *Phys. Rev. A* **28**, 2649 (1983).
- 25 D. L. Andrews, G. A. Jones, A. Salam, and R. G. Woolley, *J. Chem. Phys.* **148**, 040901 (2018).
- 26 J. Feist, A. I. Fernández-Domínguez, and F. J. García-Vidal, *Nanophotonics* **10**, 477 (2020).
- 27 J. Fregoni, F. J. García-Vidal, and J. Feist, *ACS Photonics* **9**, 1096 (2022).
- 28 R. G. Woolley, *Phys. Rev. Res.* **2**, 013206 (2020).
- 29 J. Keeling, *J. Phys.: Condens. Matter* **19**, 295213 (2007).
- 30 D. De Bernardis, P. Pilar, T. Jaako, S. De Liberato, and P. Rabl, *Phys. Rev. A* **98**, 053819 (2018).
- 31 A. Stokes and A. Nazir, *Nat. Commun.* **10**, 499 (2019).

- ³²C. Sánchez Muñoz, F. Nori, and S. De Liberato, *Nat. Commun.* **9**, 1924 (2018).
- ³³O. Di Stefano, A. Settineri, V. Macri, L. Garziano, R. Stassi, S. Savasta, and F. Nori, *Nat. Phys.* **15**, 803 (2019).
- ³⁴M. A. D. Taylor, A. Mandal, W. Zhou, and P. Huo, *Phys. Rev. Lett.* **125**, 123602 (2020).
- ³⁵J. Flick, M. Ruggenthaler, H. Appel, and A. Rubio, *Proc. Natl. Acad. Sci.* **114**, 3026 (2017).
- ³⁶E. W. Fischer and P. Saalfrank, *J. Chem. Phys.* **154**, 104311 (2021).
- ³⁷L. Garziano, A. Settineri, O. Di Stefano, S. Savasta, and F. Nori, *Phys. Rev. A* **102**, 023718 (2020).
- ³⁸V. Rokaj, D. M. Welakuh, M. Ruggenthaler, and A. Rubio, *J. Phys. B: At., Mol., Opt. Phys.* **51**, 034005 (2018).
- ³⁹C. Schäfer, M. Ruggenthaler, V. Rokaj, and A. Rubio, *ACS Photonics* **7**, 975 (2020).
- ⁴⁰P. Forn-Díaz, J. Lisenfeld, D. Marcos, J. J. García-Ripoll, E. Solano, C. J. P. M. Harmans, and J. E. Mooij, *Phys. Rev. Lett.* **105**, 237001 (2010).
- ⁴¹S.-P. Wang, G.-Q. Zhang, Y. Wang, Z. Chen, T. Li, J. S. Tsai, S.-Y. Zhu, and J. Q. You, *Phys. Rev. Appl.* **13**, 054063 (2020).
- ⁴²S. Y. Buhmann, *Dispersion Forces I: Macroscopic Quantum Electrodynamics and Ground-State Casimir, Casimir-Polder and van der Waals Forces*, Springer Tracts in Modern Physics (Springer, Berlin, Heidelberg, 2013).
- ⁴³J. Aldegunde and A. Salam, *Mol. Phys.* **113**, 226 (2015).
- ⁴⁴A. D. Dunkelberger, R. B. Davidson, W. Ahn, B. S. Simpkins, and J. C. Owrtusky, *J. Phys. Chem. A* **122**, 965 (2018).
- ⁴⁵A. D. Dunkelberger, A. B. Grafton, I. Vurgaftman, Ö. O. Soykal, T. L. Reinecke, R. B. Davidson, B. S. Simpkins, and J. C. Owrtusky, *ACS Photonics* **6**, 2719 (2019).
- ⁴⁶R. F. Ribeiro, A. D. Dunkelberger, B. Xiang, W. Xiong, B. S. Simpkins, J. C. Owrtusky, and J. Yuen-Zhou, *J. Phys. Chem. Lett.* **9**, 3766 (2018).
- ⁴⁷R. Duan, J. N. Mastron, Y. Song, and K. J. Kubarych, *J. Phys. Chem. Lett.* **12**, 11406 (2021).
- ⁴⁸J. F. Triana and F. Herrera, [chemRxiv:10.26434/chemrxiv-2023-x82w3-v2](https://chemrxiv.org/10.26434/chemrxiv-2023-x82w3-v2) (2023).
- ⁴⁹M. Ostmann, J. Minář, M. Marcuzzi, E. Levi, and I. Lesanovsky, *New J. Phys.* **19**, 123015 (2017).
- ⁵⁰M. Born and V. Fock, *Z. Phys.* **51**, 165 (1928).
- ⁵¹X. Li, M. Bamba, Q. Zhang, S. Fallahi, G. C. Gardner, W. Gao, M. Lou, K. Yoshioka, M. J. Manfra, and J. Kono, *Nat. Photonics* **12**, 324 (2018).
- ⁵²S. Mondal, D. S. Wang, and S. Keshavamurthy, *J. Chem. Phys.* **157**, 244109 (2022).
- ⁵³D. P. Craig and T. Thirunamachandran, *Molecular Quantum Electrodynamics: An Introduction to Radiation-Molecule Interactions*, Dover Books on Chemistry Series (Dover Publications, 1998).
- ⁵⁴C. Fábri, A. Csehi, G. J. Halász, L. S. Cederbaum, and Á. Vibók, *AVS Quantum Sci.* **6**, 023501 (2024).
- ⁵⁵H.-J. Werner, P. J. Knowles, G. Knizia, F. R. Manby, M. Schütz *et al.*, *MOLPRO, version 2018, a package of ab initio programs*, 2018, <https://www.molpro.net>.
- ⁵⁶J. F. Triana, D. Peláez, and J. L. Sanz-Vicario, *J. Phys. Chem. A* **122**, 2266 (2018).
- ⁵⁷T. S. Rose, M. J. Rosker, and A. H. Zewail, *J. Chem. Phys.* **91**, 7415 (1989).
- ⁵⁸H.-D. Meyer, U. Manthe, and L. S. Cederbaum, *Chem. Phys. Lett.* **165**, 73 (1990).
- ⁵⁹U. Manthe, H.-D. Meyer, and L. S. Cederbaum, *J. Chem. Phys.* **97**, 3199 (1992).
- ⁶⁰M. Beck, A. Jackle, G. Worth, and H.-D. Meyer, *Phys. Rep.* **324**, 1 (2000).
- ⁶¹A. D. Hammerich, U. Manthe, R. Kosloff, H.-D. Meyer, and L. S. Cederbaum, *J. Chem. Phys.* **101**, 5623 (1994).
- ⁶²A. Raab, G. A. Worth, H.-D. Meyer, and L. S. Cederbaum, *J. Chem. Phys.* **110**, 936 (1999).
- ⁶³O. Vendrell, F. Gatti, and H.-D. Meyer, *J. Chem. Phys.* **127**, 184303 (2007).
- ⁶⁴O. Vendrell, *Chem. Phys.* **509**, 55 (2018).
- ⁶⁵J. F. Triana and J. L. Sanz-Vicario, *Phys. Rev. Lett.* **122**, 063603 (2019).
- ⁶⁶J. F. Triana and F. Herrera, *New J. Phys.* **24**, 023008 (2022).
- ⁶⁷C. Fábri, A. G. Császár, G. J. Halász, L. S. Cederbaum, and Á. Vibók, *J. Chem. Phys.* **160**, 214308 (2024).
- ⁶⁸J. F. Triana and F. Herrera, *J. Chem. Phys.* **157**, 194104 (2022).
- ⁶⁹D. E. Mann, B. A. Thrush, D. R. Lide, J. J. Ball, and N. Acquista, *J. Chem. Phys.* **34**, 420 (1961).
- ⁷⁰W. Ahn, J. F. Triana, F. Recabal, F. Herrera, and B. S. Simpkins, *Science* **380**, 1165 (2023).
- ⁷¹R. J. Sension, A. Z. Szarka, and R. M. Hochstrasser, *J. Chem. Phys.* **97**, 5239 (1992).
- ⁷²T. Jaako, Z.-L. Xiang, J. J. García-Ripoll, and P. Rabl, *Phys. Rev. A* **94**, 033850 (2016).
- ⁷³J. J. García-Ripoll, B. Peropadre, and S. De Liberato, *Sci. Rep.* **5**, 16055 (2015).
- ⁷⁴G. Diaz-Camacho, A. Bermudez, and J. J. García-Ripoll, *Phys. Rev. A* **93**, 43843 (2016).
- ⁷⁵E. Sánchez-Burillo, L. Martín-Moreno, J. J. García-Ripoll, and D. Zueco, *Phys. Rev. Lett.* **123**, 013601 (2019).
- ⁷⁶F. Herrera and F. C. Spano, *Phys. Rev. Lett.* **116**, 238301 (2016).
- ⁷⁷F. Herrera and F. C. Spano, *Phys. Rev. A* **95**, 053867 (2017).
- ⁷⁸F. Herrera and F. C. Spano, *ACS Photonics* **5**, 65 (2018).
- ⁷⁹D. Xu and J. Cao, *Front. Phys.* **11**, 110308 (2016).
- ⁸⁰M. Autore, P. Li, I. Dolado, F. J. Alfaro-Mozaz, R. Esteban, A. Atxabal, F. Casanova, L. E. Hueso, P. Alonso-González, J. Aizpurua, A. Y. Nikitin, S. Vélez, and R. Hillenbrand, *Light: Sci. Appl.* **7**, 17172 (2018).
- ⁸¹M. Lednev, F. J. García-Vidal, and J. Feist, *Phys. Rev. Lett.* **132**, 106902 (2024).
- ⁸²D. G. Baranov, B. Munkhbat, E. Zhukova, A. Bisht, A. Canales, B. Rousseaux, G. Johansson, T. J. Antosiewicz, and T. Shegai, *Nat. Commun.* **11**, 2715 (2020).
- ⁸³D. Yoo, F. de León-Pérez, M. Pelton, I.-H. Lee, D. A. Mohr, M. B. Raschke, J. D. Caldwell, L. Martín-Moreno, and S.-H. Oh, *Nat. Photonics* **15**, 125 (2021).